**ORIGINAL ARTICLE**

# Application of Fluorescence Spectroscopy in Wheat Crop: Early Disease Detection and Associated Molecular Changes

Babar Manzoor Atta[1] · Muhammad Saleem[1] · Hina Ali[1] · Muhammad Bilal[1] · Muhammad Fayyaz[2]

## Abstract

The application of fluorescence spectroscopy combined with chemometrics was explored in the current study for the detection of stripe rust in wheat. The healthy and stripe rust leaves were collected from the disease screening nursery. The variations in the blue-green region and chlorophyll fluorescence intensity in leaves provides the basis for the detection of stripe rust infection. With the progress of disease, the variations in the synchronous fluorescence spectroscopy (SFS) spectrum was witnessed. SFS is an excellent tool for the simultaneous measurement of multiple compound samples, in case of plants it generates evidence regarding the occurrence of leaf fluorophore bands thus revealing the biochemical variations going on at different infection stages. Based on the results of the current study, it is inferred that p-coumaric acid has the highest intensity in healthy samples followed by the asymptomatic leaf samples, whereas the band intensity of α-tocopherol, sinapic acid, chlorogenic acid, ferulic acid, tannins, flavonoid, carotenoids and anthocyanins increases in the diseased and the asymptomatic samples accordingly to the rust infection. Principal component analysis (PCA) beautifully differentiated the healthy and the infected leaf samples. It is evident that the asymptomatic samples are grouped with the diseased samples or independently; indicating the start of disease infection, the decision that is hard to make with the visual assessments. The results of the current study suggest that the fluorescence emission and the SFS spectral signatures acquired for stripe rust could be utilized as fingerprints for early disease detection.

**Keywords** Chlorophyll · Early detection · Leaf fluorophores · Polyphenols · Principal component analysis · Stripe rust · Synchronous fluorescence spectroscopy · Wheat

## Introduction

Wheat is the most important staple food crop [1] and is most extensively grown crop that provides 20 percent of daily protein/calories intake for 4.5 billion people around the globe [2]. The predicted global population in 2050 is 9 billion, to meet the expected increased demand of 60 percent, the annual wheat yield must increase from the current level of 1% to at least 1.6% [2]. The major constraint to the global wheat production is biotic stresses which mainly includes the wheat rusts. The three rusts of wheat namely; stripe (yellow) rust, leaf (brown) rust and stem (black) rust are most feared ones due to the rapidity with which they spread and devastate the crop. According to Ali et al. [3] all the three rusts are distributed globally and cause massive losses in different environments favoring disease epidemics. Although, stripe rust is the most destructive cereal rust compared to the leaf and stem rusts [4] and it has been witnessed as a rising problem with worldwide recurrent invasions due to combination of various factors including high migration and mutation capacity, adaptability, presence of recombinant & diverse nature of populations and development of new variants via sexual cycle [3]. The stripe rust of wheat is caused by *Puccinia striiformis* f.sp. *tritici*, which is an airborne biotrophic fungal pathogen [5]. This disease has the capability of fast spreading to the new regions and crop cultivars [6]. The stripe rust fungus grows on the plant leaves and produce elongated lesions (stripes) of yellow-orange spores, thus reducing the photosynthetic area

✉ Babar Manzoor Atta
  babar_niab@hotmail.com

[1] Agri. & Biophotonics Division, National Institute of Lasers and Optronics College, Pakistan Institute of Engineering and Applied Sciences, Nilore, Islamabad 45650, Pakistan

[2] Crop Diseases Research Institute (CDRI), National Agricultural Research Centre (NARC), Park Road, Islamabad 44000, Pakistan

and sugar production [4]. All the plant growth stages are susceptible to the infection. Yield losses ranges from negligible to complete, depending upon the wheat variety and the disease incidence.

In Pakistan, rust diseases can threaten the production of wheat crop when appear in epidemic, as happened in 1977-78 and 1989-90 when leaf and stripe rusts caused huge economic losses. The Himalayan region of Pakistan has been identified as the center of diversity and the center of origin for stripe rust, where it is developing the new races on its alternate host *Berberis vulgaris* [5–7]. The practical and economical solution to avoid losses caused by rust diseases is the cultivation of resistant wheat varieties. Due to the mutation ability, new races of rust continue to develop causing breakdown of resistant genes as witnessed in leading wheat varieties; Inqlab-91, Sehar-06 and Galaxy-13 of Pakistan. As a result, the resistant varieties are becoming susceptible; leading to higher disease incidences each year. Thus, it is imperative to detect the disease as early as possible to deploy the preventive control measures. Fungicide treatment is warranted for the control of stripe rust if 2–5% disease develops on a susceptible variety [4]. Hence, the early disease detection will assist in the timely application of the fungicides.

Mostly the leaf infections are determined using the polymerase chain reaction (PCR) based techniques, where single step mistake leads to the false results [8]. These techniques including wet chemical approaches are time taking, labor intensive and costly as well which makes their large-scale application practically impossible [9]. To overcome the shortcomings of PCR and visual assessments the scientists have used the alternate methods that includes the non-invasive and non-destructive optical techniques [10–12]. Fluorescence and Raman spectroscopy are the commonly used techniques. The higher sensitivity and specificity rate of fluorescence spectroscopy makes it a promising diagnostic tool [13] and can be used in plants to monitor; physiological state, health, nutrient/ environmental stresses and diseases [9, 14].

Several studies have been reported assessing the suitability of fluorescence spectroscopy for the detection of rust diseases in wheat [15–24] but no study encompassing the use of synchronous fluorescence spectroscopy (SFS) has been reported for early diagnosis of rust infections and the associated molecular changes. The aims of current paper are to; (i) explore the opportunity to identify the stripe rust in wheat with no visible signs of disease by using the fluorescence emission spectrum and the SFS, (ii) assess the molecular changes going on in the leaves in response to the onset of disease incidence. Significance of the current work include assisting the plant breeders in saving time and efficiently selecting the resistant genotypes at an early stage when the symptoms are not visible and to deploy control measures to stop more damage to the crop and this will also curtail financial losses to the farmers.

## Materials and Methods

The current study was designed to assess the leaves from wheat plants that are healthy, with no visible disease symptoms and with visible symptoms of disease for the detection of stripe rust by employing the fluorescence spectroscopy.

### Collection of Leaf Samples

The healthy and stripe rust leaves were collected from the disease screening nursery of Crop Diseases Research Institute (CDRI) at National Agricultural Research Centre (NARC), Islamabad. The samples were acquired on 29th and 43rd day after spraying (DAS) the inoculum on 5th and 19th March 2019, respectively. The leaves were harvested from the random plants of susceptible wheat variety 'Morocco' sown during mid-November, 2018. The healthy, asymptomatic and symptomatic (with stripe rust symptoms) leaf samples were collected for this investigation. These leaves cover the range of stripe rust disease incidence. The leaves that were infected, leaves next to the infected ones that looked visually healthy (asymptomatic) and the fresh healthy leaves were used for the collection of leaf samples from the field. To retain the freshness, leaves were kept in sealable plastic bags and transported in the ice box esky.

### Acquisition of Fluorescence Spectral Data

Fluorescence spectrum of healthy and stripe rust diseased leaf samples were recorded using; Front face fluorescence spectroscopy and Synchronous fluorescence spectroscopy (SFS). In Front face fluorescence spectroscopy the excitation source was fixed at 410 nm and emission at 420–800 nm [9], whereas in SFS both the monochromators (excitation and emission) are scanned synchronously by maintaining a fixed wavelength offset 'Δλ' between them [25, 26]. SFS was performed at the same point of the leaf samples with excitation set at 200–800 nm and scanned the offsets Δλ 10, 20, 30……100 nm, where 40 offsets displayed better results in the healthy leaf samples. All the subsequent leaf samples were analyzed by keeping the excitation wavelength of 410 nm (420–800 nm emission) and SFS excitation wavelength of 200–800 nm with 40 offsets (240–840 nm emission). For each sample five spectra were recorded by keeping 30 s time delay between spectra. Automatic Spectrofluorometer system (Fluoromax-4, Horiba Instruments INC., NJ, USA) [9, 25] was used to record the spectral data of the leaf samples in front face format. The spectral data was normalized and displayed in the figures. The fluorescence spectral data of wheat leaf samples were processed and analyzed with the software OriginPro (version 2018).

## Principal Component Analysis (PCA)

PCA is probably the best technique of multivariate analysis with the core idea to reduce dimensionality in the large variables data set while keeping maximum variation by transposing into new set of unrelated variables known as principal components (PCs), among which initial few hold maximum variability [27]. PCA reduces the complexities from the data while retaining the trends and patterns [28] and display the similarity pattern among observations and variables as points in the graphs [29]. PCA was performed on fluorescence spectral data to visualize the grouping of leaf samples based on the similarities and differences.

## Results and Discussion

The stripe rust susceptible wheat variety 'Morocco' [30, 31] was used in the present investigation. The fluorescence emission and the synchronous spectrum analysis have been described here.

### Fluorescence Spectroscopy of Stripe Rust

The fluorescence emission spectra of healthy and stripe rust wheat leaves collected on 29th and 43rd day after spray (DAS) at 440 to 800 nm range are presented (Figs. 1 and 2). Green leaves of plants produce two classes of fluorescence i.e. blue-green fluorescence (400–600 nm) and chlorophyll fluorescence (650–800 nm) [9, 13]. On both the dates, the major fluorescence peaks are displayed at 450, 465, 480, 520–560, 680 and 730 nm (Figs. 1 and 2). These bands have been reported earlier in bacterial leaf blight of rice and citrus canker in citrus species (grape fruit and Mexican lime) along with

their molecular assignments by Atta et al. [9, 32]. The bands at 400–600 nm represent numerous leaf fluorophores including hydroxycinnamic acids, flavonols, isoflavones, flavanones, phenolic acids [33] and some secondary metabolites i.e. ferulic acid, flavonoids, coumarin, quercetin involved in plant protection system [8] and hydrocarbon carotenes (violaxanthin and antheraxanthin) [10]. At 680 and 730 nm wavelength are the characteristic emission peaks of 'chlorophyll a' [8–10, 14, 32–37]. The red and far-red fluorescence is emitted from Chlorophyll a of the antenna system of photosystem II in the thylakoids of chloroplasts of green mesophyll cells [38].

The leaf samples in the current study cover the range of stripe rust disease incidence starting from a very early disease when the symptoms are not visible to the naked eye ranged to the 100% disease incidence. The blue-green spectral region and the red-far-red chlorophyll fluorescence regions depicted in Figs. 1 and 2 clearly indicated the reduced chlorophyll in the asymptomatic and symptomatic leaf samples compared to the healthy leaf samples, predominantly the 730 nm band was either narrow or absent in the leaf samples with low to high disease. The 730 nm declining band distinguished the healthy and the infected samples in accordance to the chlorophyll emission spectrum. In addition, an increase has been witnessed in the blue-green fluorescence (450–570 nm) region on the onset of infection and the appearance of the disease, although healthy samples showed narrow spectra in that region. In the green (healthy) leaves the chlorophyll and carotenoids absorb the light in blue-green spectral region and hence the blue-green band is narrow. However, in the diseased leaf the chlorophyll is less and hence less absorption of light results in higher blue-green region band. The spectra of E1 leaf collected as asymptomatic sample (Fig. 1) indicated that the leaf is quite healthy and there are no signs of the start of the



**Fig. 1** Normalized emission spectra of healthy and stripe rust wheat leaves collected on 29th day after spray (DAS) with excitation wavelength of 410 nm and emission at 440–800 nm. The intensity of peaks is along y-axis
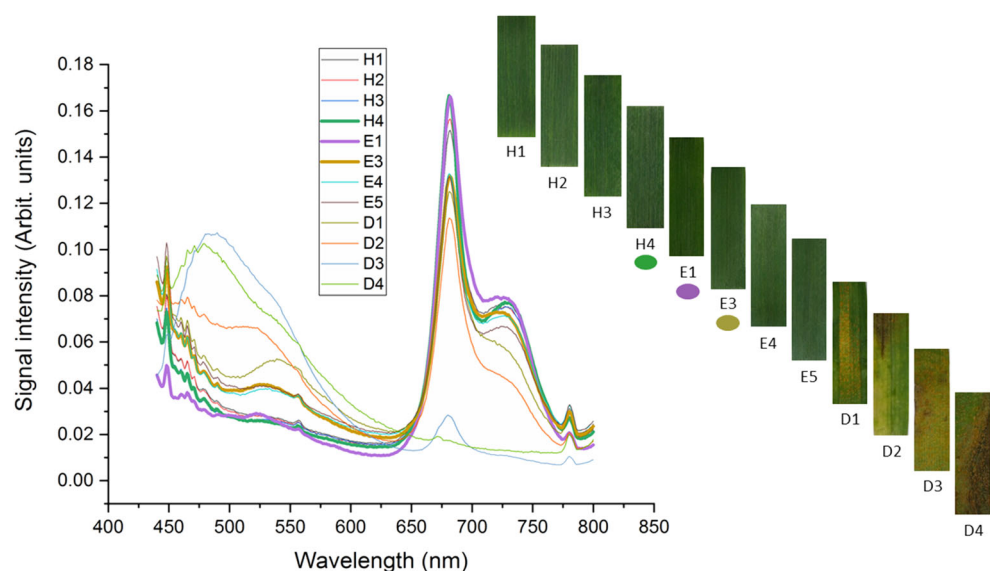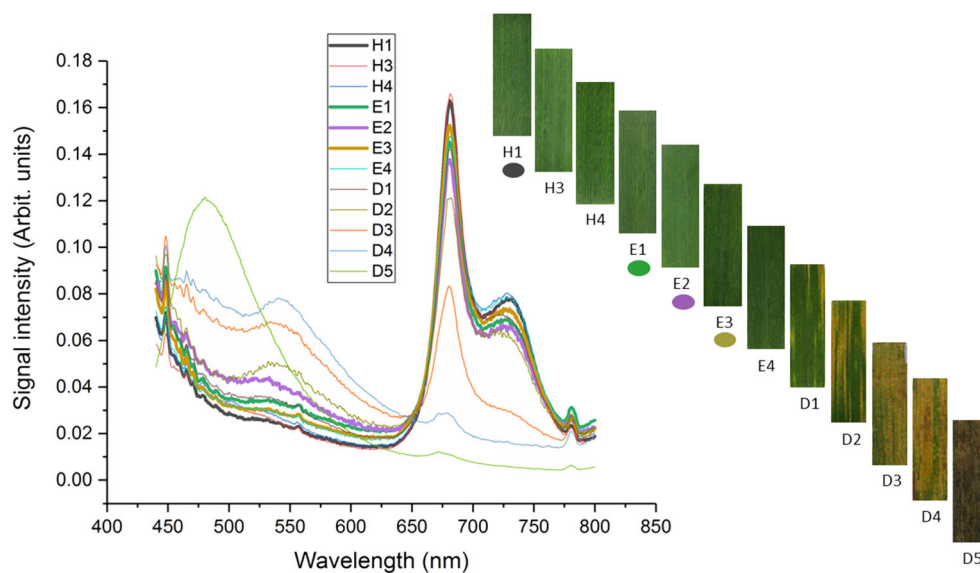
**Fig. 2** Normalized emission spectra of healthy and stripe rust wheat leaves collected on 43rd day after spray (DAS) with excitation wavelength of 410 nm and emission at 440–800 nm. The intensity of peaks is along y-axis

disease. Whereas, the other asymptomatic samples; E3, E4 & E5 (Fig. 1) and E1, E2 & E3 (Fig. 2) showed a decline in the intensity of 630 and 730 nm chlorophyll bands along with a rise in the blue-green region.

Chlorophyll is an essential component of plant leaf, in case of biotic or abiotic stress its content changes and could be observed by changes in fluorescence at the initial phase when symptoms are undetectable. In the present investigation, decrease in chlorophyll fluorescence and an increase in blue-green spectral region provides a tool for predicting stripe rust at an early stage. In response to stress the decrease of chlorophyll bands at 680 and 730 nm coupled with the increase of 450–560 nm bands is in conformity to the earlier reports [8, 14, 22, 39]. The spectral analysis of leaf samples shows that higher chlorophyll reduction from lower to higher direction has been witnessed in samples; D1 to D4 (Fig. 1) and D1 to D5 (Fig. 2), proportionate to the hike in disease infection. Moreover, same leaf samples displayed the highest increase in the blue-green region thus expressing the infection intensity. An important finding of this study is that the asymptomatic leaf samples; E5 (Fig. 1) and E2 (Fig. 2) with no visible disease signs and the leaf samples D1 (Figs. 1 and 2) with the noticeable disease signs displayed nearly the similar trend of chlorophyll and blue-green region spectral variations. Thus, it has been concluded that the prediction of disease infection at an early can be achieved by using the fluorescence signatures of chlorophyll and blue-green spectral regions.

The fluorescence ratios have been used by the researchers for fluorescence spectral analysis of leaves & plant disease detection [20, 21, 40–43] and also recommended for remote sensing [15]. Figure 3 shows the fluorescence ratios; BF/GF (F450/F530), BF/RF (F450/F685), GF/RF (F530/F685) and GF/FRF (F530/F730) of healthy and infected wheat leaves in dependence of the degree of stripe rust infection. The fluorescence ratio F450/F530 decreases with the increase in fungal infection whereas for the ratios F450/F685, F530/F685 and F530/F730 an increase with increase in fungal infection (Fig. 3) was observed due to the pronounced blue and green fluorescence of the fungus [15]. As found in the current study and reported earlier the healthy and infected wheat genotypes can be discriminated by using these fluorescence ratios [20].

The PCA scatter plot of healthy and stripe rust wheat leaves collected on 29th DAS is presented in Fig. 4. The first two principal components (PCs) accounted for 97.7% variation in the data. PCA superbly separated the healthy, asymptomatic and symptomatic leaf samples. It has been witnessed through emission spectra and also noticed here that the E1 sample has been grouped with the healthy samples, representing the healthy nature of leaf with no disease initiation. The asymptomatic leaf samples (E3, E4 and E5) have been clustered together in a separate quadrant revealing the initiation of disease infection and the start of biochemical changes; the prediction which cannot be made through visual inspection. The diseased samples have been arranged on the basis of their disease intensity. The target group is the asymptomatic leaf samples that should be well-considered for detection of disease infection at the early stage.

The PCA scatter plot of healthy and stripe rust wheat leaves collected on 43rd DAS is presented in Fig. 5. The PC1 and PC2 accounted for 98% variation in the spectral data. Like earlier, PCA nicely separated three classes of leaf samples. It is worthy noticeable that the asymptomatic (E1, E2 and E3) and the symptomatic (D1) samples have been grouped together (Fig. 5) enlightening the fact that disease infection has been started. The other symptomatic samples are arranged with respect to their disease intensity.

The combined PCA scatter plot of healthy and stripe rust wheat leaves collected on 29th and 43rd DAS has been

**Fig. 3** Fluorescence ratios of healthy and stripe rust wheat leaves collected on 29th DAS
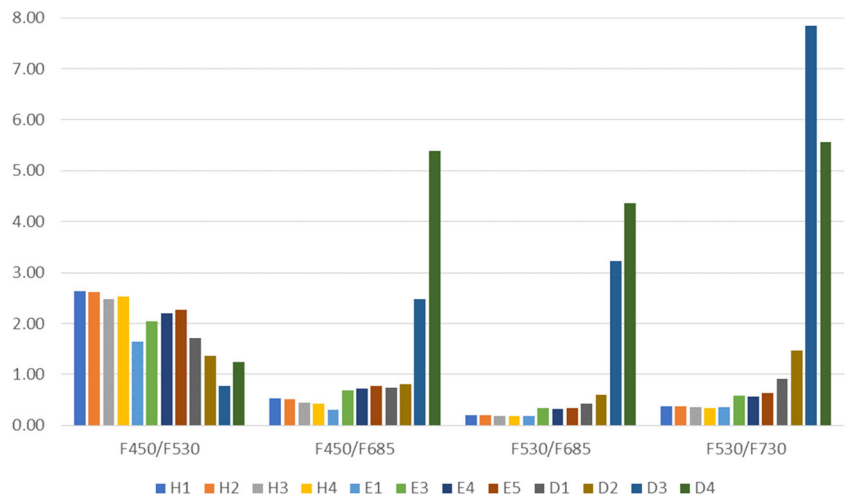


presented in Fig. 6. The PC1 and PC2 contributed 97% of variation in data. PCA beautifully grouped different leaf classes based on the health and the disease infection. It is evident that the fluorescence emission spectroscopy combined with the chemometrics successfully detected the stripe rust disease initiation at the early stage in wheat crop.

## Synchronous Fluorescence Spectroscopy (SFS) of Stripe Rust

SFS is an efficient tool for the simultaneous measurements of multi-compound samples and also deliver some significant advantages i.e. spectral simplification, narrowing of bandwidth, scattering interference reduction, improvement in analytical selectivity and enhanced resolution [26]. The SFS technique is flexible in probing various fluorophores by a suitable choice of $\Delta\lambda$ values [44]. The untreated healthy control was studied in parallel to associate the enhanced production of

polyphenols to the fungal infection [23]. In plants the phenolic compounds and the chlorophyll content changes over time, in order to tackle this issue, all the leaf samples were collected at same time on that particular date. Each SFS emission band identified in the leaf samples collected on 29th and 43rd DAS have been discussed simultaneously in the following paragraphs.

The synchronous fluorescence emission spectrum of wheat leaf samples were acquired at excitation wavelength of 200–800 nm with $\Delta\lambda = 40$ nm. The relative band intensities at wavelength range 240–840 has been displayed (Figs. 7 and 8). The prominent emission band with maximal peak intensity at 325 nm represent the $\alpha$-tocopherol. The presence of $\alpha$-tocopherol has been reported in wheat leaves [45, 46] and grains [47, 48]. Basically tocopherols are lipid-soluble antioxidants, generally known as Vitamin E [49]. Interestingly in our daily diet, the $\alpha$-tocopherol is a much active and required form of vitamin E [50]. In the present study the $\alpha$-tocopherol has
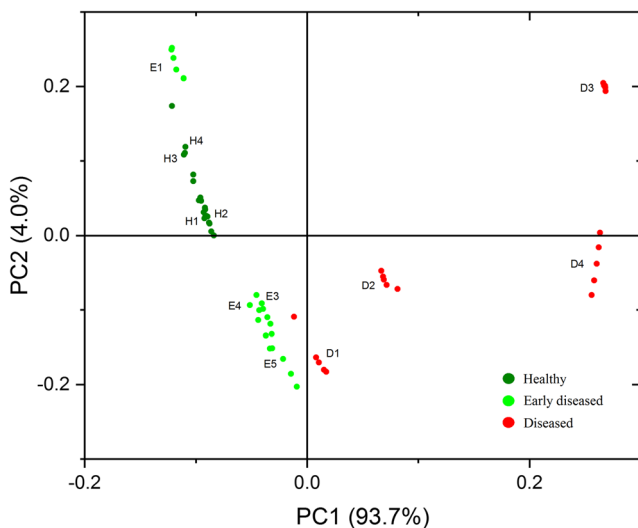


**Fig. 4** PCA scatter plot of healthy and stripe rust wheat leaves collected on 29th DAS using the emission data at 440–800 nm
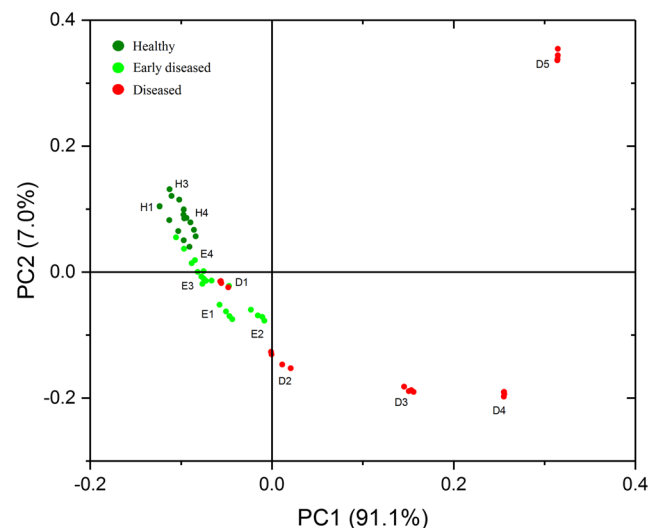


**Fig. 5** PCA scatter plot of healthy and stripe rust wheat leaves collected on 43rd DAS using the emission data at 440–800 nm
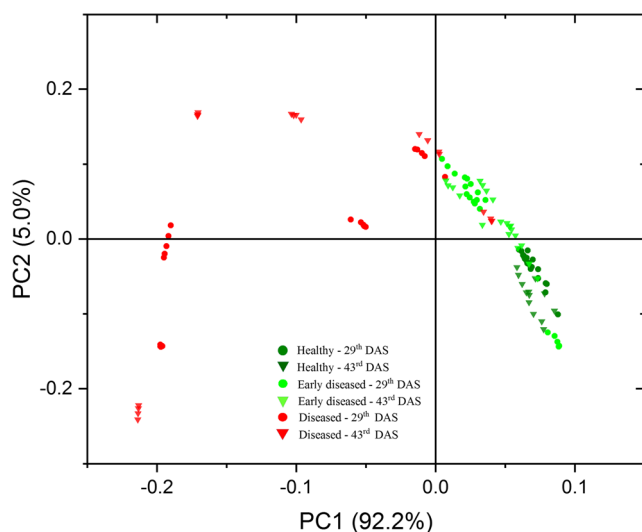
Fig. 6 PCA scatter plot of healthy and stripe rust wheat leaves collected on 29th and 43rd DAS using the emission data at 440–800 nm



Fig. 8 Normalized synchronous emission spectra of healthy and stripe rust wheat leaves collected on 43rd DAS at excitation wavelength of 200–800 nm and $\Delta\lambda = 40$ nm (emission 240–840 nm)

been found to be at the same level in all the healthy, whereas higher intensity has been observed in the asymptomatic (E3 & E4) and maximum in the symptomatic (D1, D3, & D4) leaf samples (Fig. 7). Almost the same trend has been observed in the leaf samples collected on the second date (Fig. 8) except the minimum $\alpha$-tocopherol intensity observed in the leaf sample (D5) with 100% disease severity.

The major fluorescence emission band in 370–420 nm range with maximum intensity at 405 nm indicates the p-coumaric acid. Large intensity variation has been observed in this band with maximum intensity in healthy and minimum in diseased samples (Figs. 7 and 8). The reduction in the peak along with the shifting of spectra has been noticed in the asymptomatic and symptomatic leaf samples.
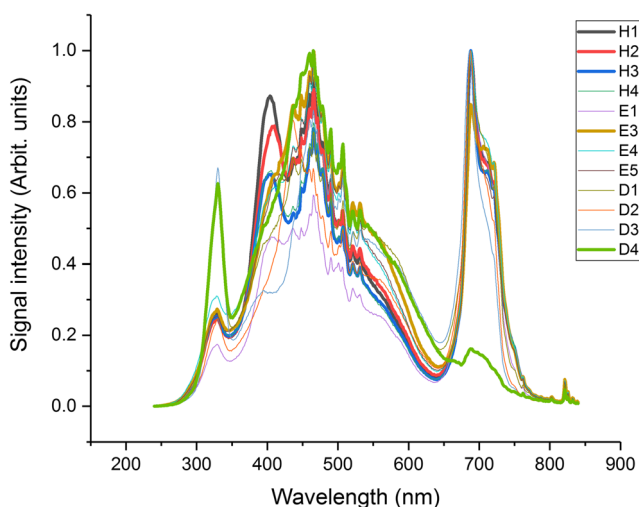


Fig. 7 Normalized synchronous emission spectra of healthy and stripe rust wheat leaves collected on 29th DAS at excitation wavelength of 200–800 nm and $\Delta\lambda = 40$ nm (emission 240–840 nm)
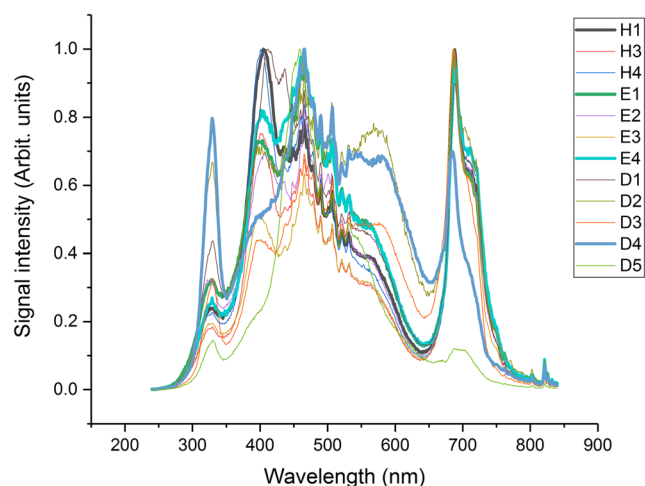
In case of wheat, the blue-green fluorescence region has been reported to be associated with several leaf fluorophores, which are identified in the current study as: sinapic acid (436 nm) [51–54]; chlorogenic acid (448 nm) [42, 47, 53]; ferulic acid (prominent peak at 465 nm) [23, 47, 48, 51–53, 55, 56]; tannins (506 nm) [57]; flavonoid (isoorientine and tricine) / flavin (522 nm) [42, 47, 53, 58, 59]; carotenoids (532 nm) [40, 45, 47, 48, 60–66]; and anthocyanins (hump at 560 nm) [67] (Figs. 7 and 8). The major peaks at 685 nm and 720 nm indicate chlorophyll bands in wheat [40, 56, 60, 61, 63, 66, 68, 69]. The fluorophores in the blue-green spectral range of 436–560 nm showed decreasing trend of the healthy leaf samples, whereas in general an increase has been noticed for asymptomatic and symptomatic samples.

The highest spectral intensity for sinapic acid, chlorogenic acid, ferulic acid, tannins, flavonoid, carotenoids and anthocyanins have been observed in the asymptomatic (E3) and highly symptomatic sample (D4), whereas the healthy samples (H3) has the lowest intensity for all the above mentioned polyphenols (Figs. 7 and 8). On the basis of these results it is inferred that p-coumaric acid has the highest intensity in healthy samples followed by the asymptomatic leaf samples, whereas the peak intensity of $\alpha$-tocopherol, sinapic acid, chlorogenic acid, ferulic acid, tannins, flavonoid, carotenoids and anthocyanins increases in the diseased and the asymptomatic samples as a result of stress which in present case is stripe rust. The blue-green region (430–580 nm) have narrow spectra for the healthy than the diseased samples. Only healthy samples displayed the prominent chlorophyll 680 and 720 nm bands. The narrowing of chlorophyll bands in the asymptomatic samples (E3, E5 Fig. 7; E4 Fig. 8) reveal the start of the disease. The elevated blue-green region coupled with the declined chlorophyll bands have been observed in the samples with highest disease. The variations in the blue-green

region and chlorophyll fluorescence intensity in wheat leaves provides the basis for the investigation of stripe rust infection stages.

Tischler et al. [23] identified from day eight the higher values of polyphenol contents in inoculated wheat plants compared to the controls. Highest intensity of phenolic compounds at 436–560 nm range coupled with the least chlorophyll has been witnessed in the severely diseased leaf samples D3, D4 (Fig. 7) and D4, D5 (Fig. 8). The key finding of this study using SFS technique being the rise in blue-green region of the infected samples and the corresponding decline in chlorophyll bands particularly in the asymptomatic leaf samples demonstrating the possibility of early detection of the disease infestation, usually hard to forecast with the visual assessments.

In winter wheat cultivars the fluorescence region between 500 and 620 nm range has been reported to be significantly increased in leaves inoculated with powdery mildew compared to the control [42]. The detected fluorescence from a leaf is largely emitted by the compounds present in the walls of epidermal cells and vascular bundles [37]. Earlier studies have revealed an association between the fungal infection and higher production of polyphenols in the host plant and this has been confirmed through HPLC analysis in wheat infected with brown rust [23]. In a plant defense mechanism, the polyphenols are synthesized because they act antibiotically in response to the fungal infection. Lichtenthaler and Schweiger [53] demonstrated that the monocotyledonous plants (wheat, oat and maize) possess many folds higher intensities of covalently bound cinnamic acids (ferulic & p-coumaric) in their cell walls of the leaves than dicotyledonous plants (spinach, sunflower and pumpkin). Higher relative amounts of ferulic acid and p-coumaric acid have been reported in wheat where ferulic acid bound in cell wall is main component of blue-green fluorescence emission [53]. Southerton and Deverall [55] identified the phenolic acids including ferulic acid, p-coumaric acid and syringic acid in the primary leaves of wheat in bound and unbound forms. The sinapic acid and chlorogenic acid exhibit fluorescence emission between 440 and 455 nm wavelength [53]. Tannins, the major polyphenol in plants, primarily function as defense compounds against biotic and abiotic stresses [70]. The tannins have been reported to fluoresce nearly at emission wavelength of 500 nm and are widely distributed and present in all plant organs [57]. The major favonoids in wheat leaves are isoorientine and tricine [59]. While working on the fluorescence emission in plants detected and quantified four flavonoids in greenhouse and ten in outdoor wheat plants [53]. The carotenes usually increase in response to fungal/disease attack or in stress, hence the increased band of carotenes can be seen in SFS spectra according to the disease intensity. Gitelson et al. [67] has reported the anthocyanins to occur at the spectral range of
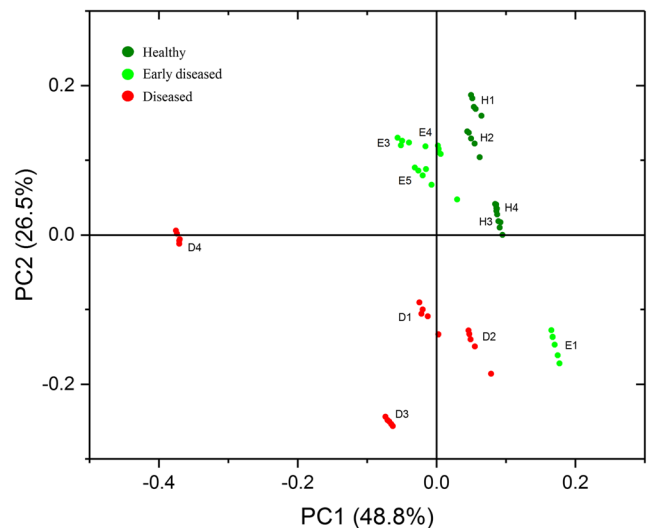


**Fig. 9** PCA scatter plot of healthy and stripe rust wheat leaves collected on 29th DAS using the synchronous emission data at 240–840 nm

540–560 nm. This colored pigment protects the plant leaves from excessive light [71, 72].

The PCA scatter plot of samples collected on 29th DAS (Fig. 9) showed 75 percent variation in the spectral data. PCA grouped the samples in the four quadrants based on their health. The healthy samples are grouped together, whereas diseased samples are arranged with respect to their disease intensity. The asymptomatic samples are grouped either separately or with the symptomatic samples and are of primary importance revealing early disease detection with SFS technique. PCA of the samples collected on 43rd DAS (Fig. 10) showed 78 percent variation in data. Similar as earlier, PCA grouped the asymptomatic samples away from the healthy samples but with the diseased sample (D1). The combined PCA for both the dates (Fig. 11) displayed the clear separation
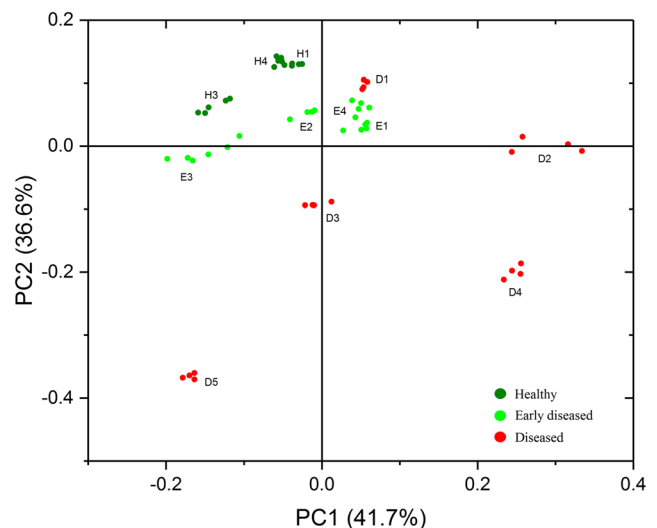


**Fig. 10** PCA scatter plot of healthy and stripe rust wheat leaves collected on 43rd DAS using the synchronous emission data at 240–840 nm
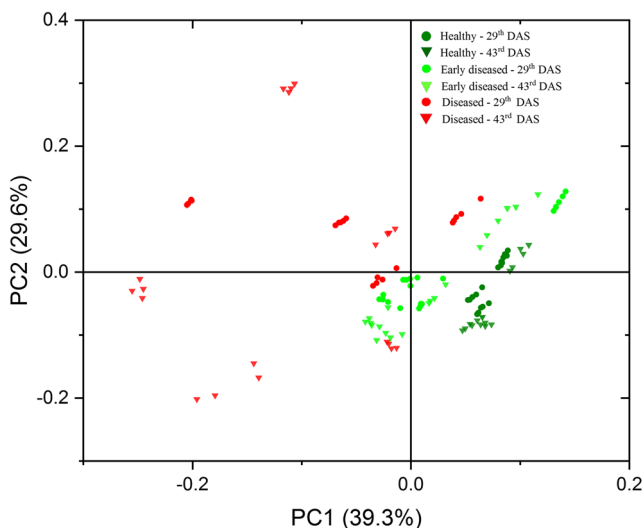
**Fig. 11** PCA scatter plot of healthy and stripe rust wheat leaves collected on 29th and 43rd DAS using the synchronous emission data at 240–840 nm

of healthy, asymptomatic and diseased samples. The synchronous fluorescence technique coupled with chemometrics successfully differentiated the early diseased samples at an initial stage.

Leufen et al. [73] probed the promise of fluorescence based optical devices to examine plant-pathogen relations in spring barley genotypes by assessing healthy leaves and leaves inoculated with powdery mildew and leaf rust. The authors were able to detect pathogen infection & disease development, distinguished between the two diseases, revealed genotype specific responses to pathogen infections and observed differences between susceptible and resistant barley cultivars. Chlorophyll fluorescence imaging sometimes offer ways to diagnose infection in divergent plant-pathogen interrelations before the detectable signs emerge by providing measureable know how regarding degree & nature of pathogen effect on the metabolism of host [18]. As a part of our ongoing research work on the early detection of different diseases in crop plants, the development of chlorophyll fluorescence imaging system is in progress to investigate disease incidence and extent on plants canopy based on the decline of chlorophyll fluorescence.

## Conclusions

Conventional methods of pigment analysis for disease detection by wet chemistry are time consuming, laborious and expensive, whereas the use of fluorescence emission spectroscopy and the SFS combined with chemometrics in the current study recognized these as a valuable and rapid approaches for detecting stripe rust in wheat. The spectral analysis revealed the differences among the wheat leaf samples. The variations

in the blue-green region and chlorophyll fluorescence intensity in leaves provides the basis for the investigation of stripe rust infection stages. It has been demonstrated that this event happens as the stripe rust develops. The use of SFS was quite advantageous as it furnished added evidence regarding the occurrence of leaf fluorophore bands, thus indicating the biochemical variations going on at different infection stages in the leaves. On the basis of the results of the current study, it is inferred that p-coumaric acid has the highest intensity in healthy samples followed by the asymptomatic leaf samples, whereas the peak intensity of α-tocopherol, sinapic acid, chlorogenic acid, ferulic acid, tannins, flavonoid, carotenoids and anthocyanins increases in the diseased and the asymptomatic samples based on the disease infection. PCA nicely differentiated the healthy and the infected leaf samples. The PC1 and the PC2 accounted for 70–98 percent variation in the spectral data. It is evident that the asymptomatic samples are grouped with the diseased samples or independently; highlighting the start of disease infection and thus aiding stripe rust detection at the initial stage.

## Compliance with Ethical Standards

**Conflict of Interest**   The authors declare that they have no conflict of interest.

## References

1. Shewry PR, Hey SJ (2015) The contribution of wheat to human diet and health. Food Energy Secur 4:178–202. https://doi.org/10.1002/fes3.64

2. Lucas H (2012) Breakout session P1.1 National Food Security-the wheat initiative-an international research initiative for wheat improvement. In: Second Global Conference on Agricultural Research for Development, 29 Oct. – 1 Nov. Punta del Este, Uruguay. GCARD, pp 1–3

3. Ali S, Rodriguez-Algaba J, Thach T et al (2017) Yellow rust epidemics worldwide were caused by pathogen races from divergent genetic lineages. Front Plant Sci 8:1–13. https://doi.org/10.3389/fpls.2017.01057 (article 1057).

4. WSU (2019) Stripe rust | Wheat & Small Grains | Washington State University. In: Wheat Small Grains, CAHNRS WSU Ext. http://smallgrains.wsu.edu/disease-resources/foliar-fungal-diseases/stripe-rust/. Accessed 28 Jun 2019

5. Ali S, Leconte M, Rahman H et al (2014) A high virulence and pathotype diversity of Puccinia striiformis f.sp. tritici at its centre of diversity, the Himalayan region of Pakistan. Eur J Plant Pathol 140:275–290. https://doi.org/10.1007/s10658-014-0461-2

6. Ali S, Gladieux P, Leconte M et al (2014) Origin, migration routes and worldwide population genetic structure of the wheat yellow rust pathogen Puccinia striiformis f.sp. tritici. PLoS Pathog 10:e1003903. https://doi.org/10.1371/journal.ppat.1003903

7. Ali S, Gladieux P, Rahman H et al (2014) Inferring the contribution of sexual reproduction, migration and off-season survival to the temporal maintenance of microbial populations: a case study on the wheat fungal pathogen *Puccinia striiformis* f.sp. *tritici*. Mol Ecol 23:603–617. https://doi.org/10.1111/mec.12629

8. Ranulfi AC, Cardinali MCB, Kubota TMK et al (2016) Laser-induced fluorescence spectroscopy applied to early diagnosis of citrus Huanglongbing. Biosyst Eng 144:133–144. https://doi.org/10.1016/j.biosystemseng.2016.02.010

9. Atta BM, Saleem M, Ali H et al (2018) Chlorophyll as a biomarker for early disease diagnosis. Laser Phys 28:065607. https://doi.org/10.1088/1555-6611/aab94f

10. Ullah R, Khan S, Bilal M et al (2016) Non-invasive assessment of mango ripening using fluorescence spectroscopy. Optik (Stuttg) 127:5186–5189. https://doi.org/10.1016/j.ijleo.2016.03.049

11. Kolb CA, Wirth E, Kaiser WM et al (2006) Noninvasive evaluation of the degree of ripeness in grape berries (Vitis Vinifera L Cv. Bacchus and Silvaner) by chlorophyll fluorescence. J Agric Food Chem 54:299–305. https://doi.org/10.1021/jf052128b

12. Agati G, Pinelli P, Cortés Ebner S et al (2005) Nondestructive evaluation of anthocyanins in olive (Olea europaea) fruits by in situ chlorophyll fluorescence spectroscopy. J Agric Food Chem 53:1354–1363. https://doi.org/10.1021/jf048381d

13. Kumar P, Akhtar J, Kandan A et al (2016) Advance detection techniques of phytopathogenic fungi: current trends and future perspectives. In: Kumar P, Gupta VK, Tiwari AK, Kamle M (eds) Current trends in plant disease diagnostics and management practices, fungal biology. Springer International Publishing, Switzerland, pp 265–298

14. Gouveia-neto AS, Silva-jr EA, Cunha PC et al (2011) Abiotic stress diagnosis via laser induced chlorophyll fluorescence analysis in plants for biofuel. In: Bernardes MADS (ed) Biofuel production-recent developments and prospects. InTech, Rijeka, pp 1–22

15. Lüdeker W, Dahn HG, Günther KP (1996) Detection of fungal infection of plants by laser-induced fluorescence: an attempt to use remote sensing. J Plant Physiol 148:579–585. https://doi.org/10.1016/S0176-1617(96)80078-2

16. Tartachnyk II, Rademacher I, Kühbauch W (2006) Distinguishing nitrogen deficiency and fungal infection of winter wheat by laser-induced fluorescence. Precis Agric 7:281–293. https://doi.org/10.1007/s11119-006-9008-7

17. Kuckenberg J, Tartachnyk I, Noga G (2009) Temporal and spatial changes of chlorophyll fluorescence as a basis for early and precise detection of leaf rust and powdery mildew infections in wheat leaves. Precis Agric 10:34–44. https://doi.org/10.1007/s11119-008-9082-0

18. Scholes JD, Rolfe SA (2009) Chlorophyll fluorescence imaging as tool for understanding the impact of fungal diseases on plant performance: a phenomics perspective. Funct Plant Biol 36:880–892

19. Bürling K, Hunsche M, Noga G (2010) Quantum yield of non-regulated energy dissipation in PSII (Y(NO)) for early detection of leaf rust (Puccinia triticina) infection in susceptible and resistant wheat (Triticum aestivum L.) cultivars. Precis Agric 11:703–716. https://doi.org/10.1007/s11119-010-9194-1

20. Burling K, Hunsche M, Noga G et al (2011) UV-induced fluorescence spectra and lifetime determination for detection of leaf rust (Puccinia triticina) in susceptible and resistant wheat (Triticum aestivum) cultivars. Funct Plant Biol 38:337–345. https://doi.org/10.1071/FP10171

21. Bürling K, Hunsche M, Noga G (2011) Use of blue-green and chlorophyll fluorescence measurements for differentiation between nitrogen deficiency and pathogen infection in winter wheat. J Plant Physiol 168:1641–1648. https://doi.org/10.1016/j.jplph.2011.03.016

22. Römer C, Bürling K, Hunsche M et al (2011) Robust fitting of fluorescence spectra for pre-symptomatic wheat leaf rust detection with Support Vector Machines. Comput Electron Agric 79:180–188. https://doi.org/10.1016/j.compag.2011.09.011

23. Tischler YK, Thiessen E, Hartung E (2018) Early optical detection of infection with brown rust in winter wheat by chlorophyll fluorescence excitation spectra. Comput Electron Agric 146:77–85. https://doi.org/10.1016/j.compag.2018.01.026

24. Firdous S (2018) Optical fluorescence diagnostic of wheat leaf rust with laser scanning confocal microscopy. Adv Crop Sci Technol 06:2–5. https://doi.org/10.4172/2329-8863.1000355

25. Ullah R, Khan S, Ali H et al (2017) Identification of cow and buffalo milk based on Beta carotene and vitamin-A concentration using fluorescence spectroscopy. PLoS One 12:1–10. https://doi.org/10.1371/journal.pone.0178055

26. Li Y-Q, Li X-Y, Shindi AAF et al (2012) Synchronous fluorescence spectroscopy and its applications in clinical analysis and food safety evaluation. In: Geddes CD (ed) Reviews in Fluorescence 2010. Springer, New York, pp 95–117

27. Jolliffe IT (2002) Principal component analysis, second edition. Encycl Stat Behav Sci 30:487. https://doi.org/10.2307/1270093

28. Lever J, Krzywinski M, Altman N (2017) Points of Significance: principal component analysis. Nat Methods 14:641–642. https://doi.org/10.1038/nmeth.4346

29. Abdi H, Williams LJ (2010) Principal component analysis. Wiley Interdiscip Rev Comput Stat 2:433–459. https://doi.org/10.1002/wics.101

30. Saleem K, Arshad HMI, Shokat S, Atta BM (2015) Appraisal of wheat germplasm for adult plant resistance against stripe rust. J Plant Prot Res 55:405–414. https://doi.org/10.1515/jppr-2015-0055

31. Ali S, Shah SJA, Rahman H (2009) Multi-location variability in Pakistan for partial resistance in wheat to Puccinia striiformis f. sp. tritici. Phytopathol Mediterr 48:269–279. https://doi.org/10.14601/Phytopathol_Mediterr-2669

32. Atta BM, Saleem M, Ali H et al (2019) Synchronous fluorescence spectroscopy for early diagnosis of citrus canker in citrus species. Laser Phys 29. https://doi.org/10.1088/1555-6611/ab2802

33. Falco WF, Botero ER, Falcão EA et al (2011) In vivo observation of chlorophyll fluorescence quenching induced by gold nanoparticles. J Photochem Photobiol A Chem 225:65–71. https://doi.org/10.1016/j.jphotochem.2011.09.027

34. Lang M, Stober F, Lichtenthaler HK (1991) Fluorescence emission spectra of plant leaves and plant constituents. Radiat Environ Biophys 30:333–347. https://doi.org/10.1007/BF01210517

35. Buschmann C (2007) Variability and application of the chlorophyll fluorescence emission ratio red/far-red of leaves. Photosynth Res 92:261–271

36. Lagorio MG, Cordon GB, Iriel A (2015) Reviewing the relevance of fluorescence in biological systems. Photochem Photobiol Sci 14:1538–1559

37. Donaldson L, Williams N (2018) Imaging and spectroscopy of natural fluorophores in pine needles. Plants 7:1–16. https://doi.org/10.3390/plants7010010

38. Buschmann C, Langsdorf G, Lichtenthaler HK (2000) Imaging of the blue, green, and red fluorescence emission of plants: an overview. Photosynthetica 38:483–491. https://doi.org/10.1023/A:1012440903014

39. Lenk S, Gádoros P, Kocsányi L, Barócsi A (2016) Teaching laser-induced fluorescence of plant leaves. Eur J Phys 37:064003. https://doi.org/10.1088/0143-0807/37/6/064003

40. Stober F, Lichtenthaler HK (1992) Changes of the laser-induced blue, green and red fluorescence signatures during greening of etiolated leaves of wheat. J Plant Physiol 140:673–680. https://doi.org/10.1016/S0176-1617(11)81022-9

41. Stober F, Lang M, Lichtenthaler HK (1994) Blue, green, and red fluorescence emission signatures of green, etiolated, and white leaves. Remote Sens Environ 47:65–71. https://doi.org/10.1016/0034-4257(94)90129-5

42. Bürling K, Hunsche M, Noga G (2012) Presymptomatic detection of powdery mildew infection in winter wheat cultivars by laser-induced fluorescence. Appl Spectrosc 66:1411–1419. https://doi.org/10.1366/12-06614

43. Obledo-Vázquez EN, Cervantes-Martínez J (2017) Laser-induced fluorescence spectral analysis of papaya fruits at different stages of ripening. Appl Opt 56:1753–1756. https://doi.org/10.1364/AO.56.001753

44. Sikorska E, Khmelinskii IV, Sikorski M et al (2008) Fluorescence spectroscopy in monitoring of extra virgin olive oil during storage. Int J Food Sci Technol 43:52–61. https://doi.org/10.1111/j.1365-2621.2006.01384.x

45. Keleş Y, Öncel I (2002) Response of antioxidative defence system to temperature and water stress combinations in wheat seedlings. Plant Sci 163:783–790. https://doi.org/10.1016/S0168-9452(02)00213-3

46. Bartoli CG, Simontacchi M, Tambussi E et al (1999) Drought and watering-dependent oxidative stress: effect on antioxidant content in Triticum aestivum L. leaves. J Exp Bot 50:375–383

47. Žilić S, Hadži-Tašković Šukalović V, Dodig D et al (2011) Antioxidant activity of small grain cereals caused by phenolics and lipid soluble antioxidants. J Cereal Sci 54:417–424. https://doi.org/10.1016/j.jcs.2011.08.006

48. Moore J, Hao Z, Zhou K et al (2005) Carotenoid, tocopherol, phenolic acid, and antioxidant properties of Maryland-grown soft wheat. J Agric Food Chem 53:6649–6657. https://doi.org/10.1021/jf050481b

49. Fritsche S, Wang X, Jung C (2017) Recent advances in our understanding of tocopherol biosynthesis in plants: an overview of key genes, functions, and breeding of vitamin E improved crops. Antioxidants 6:99. https://doi.org/10.3390/antiox6040099

50. DellaPenna D (2005) A decade of progress in understanding vitamin E synthesis in plants. In: Journal of Plant Physiology. Elsevier GmbH, pp 729–737

51. El-Basyouni S, Towers GHN (1964) The phenolic acids in wheat: I. Changes during growth and development. Can J Biochem 42:203–210. https://doi.org/10.1139/o64-024

52. Li L, Shewry PR, Ward JL (2008) Phenolic acids in wheat varieties in the healthgrain diversity screen. J Agric Food Chem 56:9732–9739. https://doi.org/10.1021/jf801069s

53. Lichtenthaler HK, Schweiger J (1998) Cell wall bound ferulic acid, the major substance of the blue-green fluorescence emission of plants. J Plant Physiol 152:272–282. https://doi.org/10.1016/S0176-1617(98)80142-9

54. Barron C, Surget A, Rouau X (2007) Relative amounts of tissues in mature wheat (Triticum aestivum L.) grain and their carbohydrate and phenolic acid composition. J Cereal Sci 45:88–96. https://doi.org/10.1016/j.jcs.2006.07.004

55. Southerton SG, Deverall BJ (1990) Changes in phenolic acid levels in wheat leaves expressing resistance to Puccinia recondita f. sp. tritici. Physiol Mol Plant Pathol 37:437–450. https://doi.org/10.1016/0885-5765(90)90035-V

56. Meyer S, Cartelat A, Moya I, Cerovic ZG (2003) UV-induced blue-green and far-red fluorescence along wheat leaves: a potential signature of leaf ageing. J Exp Bot 54:757–769. https://doi.org/10.1093/jxb/erg063

57. García-Plazaola JI, Fernández-Marín B, Duke SO et al (2015) Autofluorescence: biological functions and technical applications. Plant Sci 236:136–145

58. Bürling K, Cerovic ZG, Cornic G et al (2013) Fluorescence-based sensing of drought-induced stress in the vegetative phase of four contrasting wheat genotypes. Environ Exp Bot 89:51–59. https://doi.org/10.1016/j.envexpbot.2013.01.003

59. Estiarte M, Penuelas J, Kimball BA et al (1999) Free-air CO2 enrichment of wheat: leaf flavonoid concentration throughout the growth cycle. Physiol Plant 105:423–433. https://doi.org/10.1034/j.1399-3054.1999.105306.x

60. Devadas R, Lamb DW, Backhouse D, Simpfendorfer S (2015) Sequential application of hyperspectral indices for delineation of stripe rust infection and nitrogen deficiency in wheat. Precis Agric 16:477–491. https://doi.org/10.1007/s11119-015-9390-0

61. Ogawa T, Inoue Y, Kitajima M, Shibata K (1973) Action spectra for biosynthesis of chlorophylls a and b and β-carotene. Photochem Photobiol 18:229–235. https://doi.org/10.1111/j.1751-1097.1973.tb06416.x

62. Richaud D, Stange C, Gadaleta A et al (2018) Identification of Lycopene epsilon cyclase (LCYE) gene mutants to potentially increase β-carotene content in durum wheat (Triticum turgidum L.ssp. Durum) through TILLING. PLoS One 13:e0208948. https://doi.org/10.1371/journal.pone.0208948

63. Tambussi EA, Casadesus J, Munné-Bosch S, Araus JL (2002) Photoprotection in water-stressed plants of durum wheat (Triticum turgidum var. durum): changes in chlorophyll fluorescence, spectral signature and photosynthetic pigments. Funct Plant Biol 29:35–44. https://doi.org/10.1071/PP01104

64. Hussain A, Larsson H, Kuktaite R et al (2015) Carotenoid content in organically produced wheat: relevance for human nutritional health on consumption. Int J Environ Res Public Health 12:14068–14083. https://doi.org/10.3390/ijerph121114068

65. Sun T, Yuan H, Cao H et al (2018) Carotenoid metabolism in plants: the role of plastids. Mol Plant 11:58–74. https://doi.org/10.1016/j.molp.2017.09.010

66. Bauriegel E, Giebel A, Geyer M et al (2011) Early detection of Fusarium infection in wheat using hyper-spectral imaging. Comput Electron Agric 75:304–312. https://doi.org/10.1016/j.compag.2010.12.006

67. Gitelson AA, Keydan GP, Merzlyak MN (2006) Three-band model for noninvasive estimation of chlorophyll, carotenoids, and anthocyanin contents in higher plant leaves. Geophys Res Lett 33: L11402. https://doi.org/10.1029/2006GL026457

68. Bauriegel E, Herppich W (2014) Hyperspectral and chlorophyll fluorescence imaging for early detection of plant diseases, with special reference to fusarium spec. infections on wheat. Agriculture 4:32–57. https://doi.org/10.3390/agriculture4010032

69. Pandey JK, Gopal R (2011) Laser-induced chlorophyll fluorescence: a technique for detection of dimethoate effect on chlorophyll content and photosynthetic activity of wheat plant. J Fluoresc 21:785–791. https://doi.org/10.1007/s10895-010-0771-5

70. Suseela V (2019) Potential roles of plant biochemistry in mediating ecosystem responses to warming and drought. In: Ecosystem Consequences of Soil Warming. Elsevier, pp 103–124

71. Gitelson AA, Zur Y, Chivkunova OB, Merzlyak MN (2002) Assessing carotenoid content in plant leaves with reflectance spectroscopy. Photochem Photobiol 75:272–281. https://doi.org/10.1562/0031-8655(2002)075<0272:ACCIPL>2.0.CO;2

72. Merzlyak MN, Chivkunova OB (2000) Light-stress-induced pigment changes and evidence for anthocyanin photoprotection in apples. J Photochem Photobiol B Biol 55:155–163. https://doi.org/10.1016/S1011-1344(00)00042-7

73. Leufen G, Noga G, Hunsche M et al (2014) Proximal sensing of plant-pathogen interactions in spring barley with three fluorescence techniques. Sensors 14:11135–11152. https://doi.org/10.3390/s140611135